

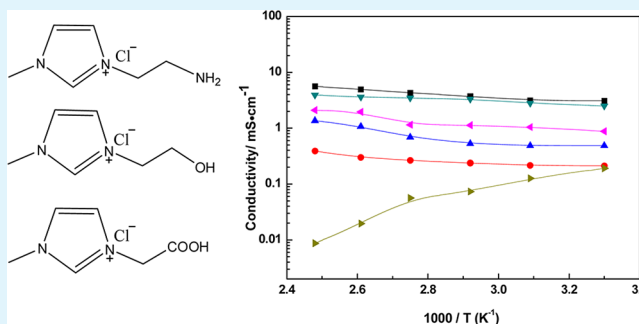
Preparation and Characterization of Nonaqueous Proton-Conducting Membranes with Protic Ionic Liquids

Fei Lu, Xinpei Gao, Xiaojun Yan, Hejun Gao, Lijuan Shi, Han Jia, and Liqiang Zheng*

Key laboratory of Colloid and Interface Chemistry, Shandong University, Ministry of Education, Jinan 250100, P. R. China

ABSTRACT: Hybrid Nafion membranes were successfully fabricated by incorporating with protic imidazolium ionic liquids 1-(2-aminoethyl)-3-methylimidazolium chloride ([MimAE]Cl), 1-(2-hydroxyethyl)-3-methylimidazolium chloride ([MimHE]Cl), and 1-carboxymethyl-3-methylimidazolium chloride ([MimCM]Cl) for high-temperature fuel cells. The composite membranes were characterized by impedance spectroscopy, small-angle X-ray scattering (SAXS), scanning electronic microscopy (SEM), and thermogravimetric analysis (TGA). The incorporated protic ionic liquids enhance the doping of phosphoric acid (PA) and result in a relatively high ionic conductivity. The Nafion/10 wt % [MimAE]Cl/PA composite membrane exhibits an ionic conductivity of 6.0 mS/cm at 130 °C without humidification. [MimAE]Cl can swell the Nafion matrix more homogeneously than [MimHE]Cl or [MimCM]Cl, which results in a better ionic conductivity. It is notable that the composite Nafion/IL/PA membranes have a better thermal stability than the pristine Nafion membranes.

KEYWORDS: protic ionic liquids, nafion, composite membranes, ionic conductivity, anhydrous condition, SAXS



INTRODUCTION

Proton-exchange membrane fuel cells (PEMFCs) are electrochemical devices to convert chemical energy into electrical power with a high efficiency and low environmental impact.^{1,2} In these fuel cells, the proton-exchange membranes (PEMs), as the central element, should exhibit high proton conductivity, good thermo-mechanical strength, low gas permeability, electro-chemical stability, and limited water swelling. Recently, various PEMs have been explored including sulfonated aromatic polymers,^{3–5} composite membranes based on inorganic fillers,^{6–9} and perfluorosulfonated ionomers.^{10–12} Because of their good performance and stability, perfluorosulfonated ionomers are the optimal material for PEMFC applications. Nafion, a perfluorosulfonated ionomer, consists of two incompatible parts: a hydrophobic polytetrafluoroethylene backbone and a hydrophilic sulfonic acid side chain. These hydrophilic acid groups allow the transportation of cations and work as ionic conductive materials. Although the composition of Nafion has been explored, there are still some drawbacks for the use of Nafion in PEMFC applications. For instance, the proton conductivity of Nafion membranes will decrease significantly at temperatures above 80 °C, which results in the evaporation of water in the membranes and thus limits proton mobility.¹³ There is a strong need for the PEMs to work at high temperatures under anhydrous conditions because the electrochemical reactions will be accelerated and the CO poisoning will be reduced as the temperature is increased.¹⁴

A new approach to increase the working temperature of Nafion is the introduction of proton-donating molecules in the Nafion membranes. Ionic liquids (ILs) with good electrical

conductivity, thermal stability, and high ion mobility are perfect candidates to improve the behavior of Nafion at high temperatures.¹⁵ Recently, a number of ILs based on alkyl ammonium have been applied to doping with Nafion, including triethylammonium,^{16–19} phenyltrimethylammonium, *n*-dodecyltrimethylammonium, hexadecyltrimethylammonium,²⁰ and others. These investigations are focused on the improvement of the electrical properties and interactions between ionic liquids and the Nafion matrix. In addition, imidazolium ILs such as 1-ethyl-3-methylimidazolium trifluoromethanesulphonate, 1-ethyl-3-methylimidazolium tetrafluoroborate,²¹ 1-butyl-3-methylimidazolium chloride, 1-butyl-3-methylimidazolium hydroxide,²² and 1-butyl-3-methylimidazolium bis-(trifluoromethylsulfonyl)imide²³ were also used to impregnate Nafion membranes. The structures of the incorporated ILs and the degree of incorporation have significant influence on the proton conductivities of the Nafion/IL composite membranes. The content of ILs doped in the Nafion membranes can be manipulated by solution-casting methods. Only low-molecular weight alcohols and organic solvents in the dispersions were evaporated because of the high boiling points of the ILs. The wide variety of ILs raises the possibility of fabricating Nafion/IL composite membranes with specific characteristics.

Another approach to improve the performance of PEMs is the incorporation of phosphoric acid (PA) with high ionic conductivity at temperatures up to 200 °C. As previously

Received: May 21, 2013

Accepted: July 16, 2013

Published: July 16, 2013

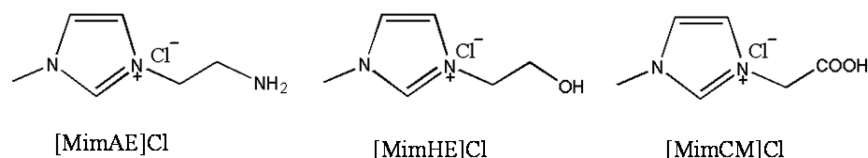


Figure 1. Chemical structures of the protic ILs.

reported, the polybenzimidazole membranes doped with PA had a good performance in PEMFCs at high temperatures under anhydrous conditions.²⁴ Many attempts were also made to fabricate PA-doped Nafion composite membranes as high-temperature proton-exchange membranes.^{25–27} He et al. have prepared composite membranes with high-temperature performance that are based on Nafion and PA.²² The obtained composite membranes exhibit an ionic conductivity of 10.9 mS/cm at 160 °C under anhydrous conditions.

In this study, composite membranes based on Nafion and protic imidazolium ILs (i.e., 1-(2-aminoethyl)-3-methylimidazolium chloride ([MimAE]Cl), 1-(2-hydroxyethyl)-3-methylimidazolium chloride ([MimHE]Cl), and 1-carboxymethyl-3-methylimidazolium chloride ([MimCM]Cl)) were fabricated by a solution-casting method. The chemical structures of the protic ILs are shown in Figure 1. The Nafion/IL membranes were then doped with PA to prepare the Nafion/IL/PA composite membranes. The electrochemical, structural, and thermal properties of the Nafion/IL/PA composite membranes were also investigated. The addition of ILs and PA can significantly improve the electrochemical properties and the thermal stability of the composite membranes.

EXPERIMENTAL SECTION

Materials. A 5 wt % Nafion solution was obtained from Sigma-Aldrich and used as received. 1-Methylimidazole (98%) was also purchased from Sigma-Aldrich and distilled prior to use. 2-Chloroethylamine hydrochloride (97%), chloroacetic acid (98%), and 2-chloroethanol (98%) were from the Xiya Reagent Company. Phosphoric acid (85%) was purchased from Tianjin Dengke Chemical Reagent Company. The purity of the products was ascertained by ¹H NMR spectrum in DMSO-*d*₆.

Synthesis of the Protic Ionic Liquids. [MimAE]Cl was prepared according to previous reports.^{28,29} Briefly, 1-methylimidazole (0.2 mol) and 2-chloroethylamine hydrochloride (0.1 mol) were dissolved in acetonitrile (150 mL), and the mixtures were heated to 70 °C under an argon atmosphere for 24 h. After the solution was cooled to room temperature, the top liquid was decanted, and the bottom solid was washed with anhydrous ethanol three times. The obtained white solid was dried under vacuum at 70 °C overnight. The resulting 1-aminoethyl-3-methylimidazolium chloride hydrochloride was dissolved in water, and the pH of the solution was adjusted to ~7.5 by the addition of KOH. After the water was removed in vacuo, the product was then separated from the ion by-product by extraction of the residue with ethanol–THF in which the imidazolium salt is soluble. The obtained IL was dried under vacuum at 70 °C for 2 days. ¹H NMR (400 MHz, DMSO-*d*₆, δ): 2.96 (t, 2H); 3.27 (br, 2H); 3.88 (s, 3H); 4.23 (t, 2H); 7.78 (s, 1H); 7.84 (s, 1H); 9.47 (s, 1H).

[MimHE]Cl was prepared according to a modified method from the literature.³⁰ Freshly distilled 1-methylimidazole (0.1 mol) and 2-chloroethanol (0.12 mol) were mixed in dry toluene (50 mL) and refluxed at 70 °C for 24 h under a nitrogen atmosphere. The mixture was cooled to room temperature to form a white solid. The product was purified by filtering followed by washing with anhydrous ether and dry MeCN. The final product was dried at 60 °C for 24 h under vacuum. ¹H NMR (400 MHz, DMSO-*d*₆, δ): 3.71 (m, 2H); 3.87 (s, 3H); 4.24 (t, 2H); 5.43 (t, 1H); 7.73 (s, 1H); 7.78 (s, 1H); 9.25 (s, 1H).

[MimCM]Cl was synthesized on the basis of a previous report.³¹ Freshly distilled 1-methylimidazole (0.1 mol) was added to a solution of chloroacetic acid (0.1 mol) in anhydrous chloroform (80 mL) at room temperature. The resulting mixture was refluxed at 70 °C for 50 h under a nitrogen atmosphere. The produced solid was filtrated and washed with anhydrous ethanol at least three times. The final product was dried at 60 °C for 24 h under vacuum. ¹H NMR (300 MHz, DMSO-*d*₆, δ): 3.90 (s, 3H); 5.16 (s, 2H); 7.73 (d, 2H); 9.15 (s, 1H); 13.75 (br, 1H).

Preparation of Composite Membranes. The preparation of composite membranes with different ionic liquids was made by a solution-casting method. A 5 wt % Nafion solution was dried at 50 °C to vaporize the solvent. The Nafion resin was dissolved in *N,N*-dimethylformamide (DMF) to form a Nafion/DMF solution. Next, the corresponding ionic liquids were added into the Nafion/DMF solution, and the mixture was stirred for 12 h to mix the ionic liquids and Nafion. The mixture was poured onto a PTFE dish, dried at 60 °C for 24 h at ambient pressure, and dried under vacuum for another 12 h. To prepare the Nafion/IL/PA composite membranes, the dry Nafion/IL membranes were dipped into concentrated phosphoric acid.

Characterization of the Composite Membranes. *Ionic Conductivity.* Conductivity measurements were performed by impedance spectroscopy in the frequency range from 100 mHz to 10 MHz with 0.01 mV oscillating voltage. The conductivity-measurement cell was placed in an oven from 30 to 130 °C for 1.5 h before each measurement. All of the conductivity measurements were performed without humidification. The ionic conductivity of each sample was calculated from the following equation²¹

$$\sigma = \frac{L}{wdR} \quad (1)$$

where σ is the ionic conductivity, L is the distance between the two electrodes of the conductivity-measurement cell, R is the membrane resistance derived from the impedance value at 0 phase angle, w is the width of the membrane, and d is the thickness of the membrane. All measurements were repeated three times to obtain the average value.

Structure and Morphology. Small-angle X-ray scattering (SAXS) measurements of the composite membranes were carried out with the SAXSess μ c² X-ray scattering system (Anton Paar). SAXS measurement was performed with a Cu $K\alpha$ radiation operating at 2 kW (50 kV and 40 mA). The distance between the sample and detector is about 264.5 mm, and the wavelength of the X-ray is 1.542 Å. The surface and cross-section morphologies of the composite membranes were investigated by scanning electronic microscopy (SEM, JEOL JSM-7600F) after gold sputter coating.

Thermal Stability. Thermo gravimetric analysis (TGA) was performed to examine the thermal stability of the composite membranes with a Rheometric Scientific TGA 1500 (Piscataway, NJ) under an inert atmosphere of nitrogen with 7 to 8 mg of the samples and a heating rate of 10 °C/min in the range from ambient temperature to 600 °C.

RESULTS AND DISCUSSION

PA-Doping Level and Ionic Conductivity of the Composite Membranes. The Nafion/IL/PA composite membranes were obtained by immersing the dried Nafion/IL membranes into concentrated phosphoric acid at room temperature. The PA-doping level of the composite membranes can vary with the type of the ILs added. Thus, an important parameter, the acid-doping level (ADL), of the Nafion/IL/PA

composite membranes should be determined. ADL, which indicates the number of H_3PO_4 molecules per mole Nafion repeated part, can be determined on the basis of the following equation²²

$$\text{ADL} = \frac{m_{\text{Nafion/IL/PA}} - m_{\text{Nafion/IL}}}{m_{\text{Nafion}}} \times \frac{1100}{98} \quad (2)$$

where m_{Nafion} , $m_{\text{Nafion/IL}}$, and $m_{\text{Nafion/IL/PA}}$ are the masses of dry Nafion, Nafion/IL, and Nafion/IL/PA membranes; 1100 is the average molecular weight of Nafion; and 98 is the molecular weight of phosphoric acid. The obtained ADL values for Nafion and Nafion/IL membranes are shown in Figure 2. All of the

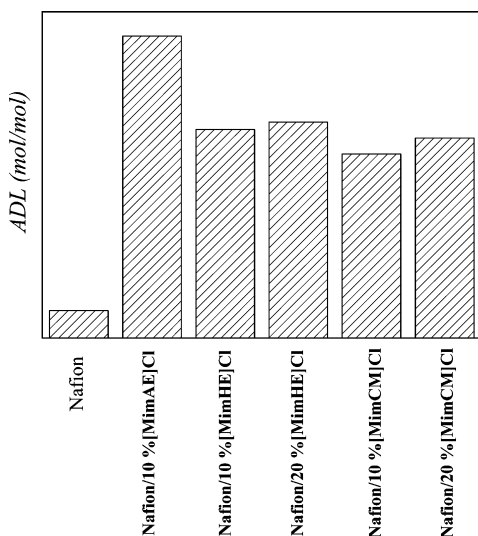


Figure 2. The acid-doping level of the Nafion and Nafion/IL composite membranes.

Nafion/IL membranes exhibit higher acid-doping levels than the pristine Nafion. Nafion incorporated with 10 wt % of the amino group functional ILs, [MimAE]Cl, was doped the most with phosphoric acid in comparison with that of Nafion/20 wt % [MimHE]Cl and Nafion/20 wt % [MimCM]Cl membranes that contain a higher content of ILs. Thus, the incorporated functional IL cations enhance the affinity of the phosphoric acid in the Nafion matrix, and the electrostatic interactions between the imidazolium cations and phosphoric acid varies with the type of the functional groups on the imidazole rings. The [MimAE]⁺ cations show the strongest electrostatic interactions with phosphoric acid resulting from the protonated amino groups. Although the electrostatic interactions between [MimCM]⁺ cations and phosphoric acid can be restricted because the carboxyl groups may release protons, the Nafion/[MimAE]Cl composite membrane can be doped the most with phosphoric acid.

Figure 3 shows the ionic conductivity of the composite membranes as function of temperature without humidification. The ionic conductivity of the Nafion/PA membrane is decreased from 0.19 to 0.0087 mS/cm when the temperature is changed from 30 to 130 °C. The main reason for the decrease in the ionic conductivity is the evaporation of water that occurs with increasing temperature and the relatively low PA-doping level. However, all the Nafion/IL/PA membranes exhibit increasing conductivity with increasing temperature. When 10 wt % of different ILs were added into Nafion, then the obtained Nafion/[MimAE]Cl/PA composite membrane

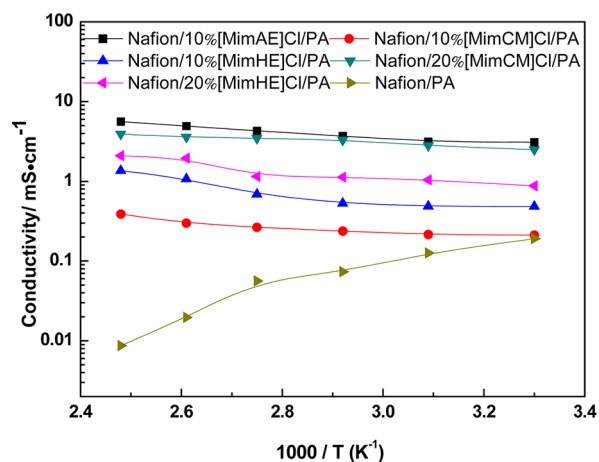


Figure 3. Conductivities of the Nafion/IL/PA composite membranes as a function of temperature with varying IL content and phosphoric acid-doped Nafion for comparison.

exhibited the highest ionic conductivity of about 6.0 mS/cm at 130 °C, whereas the ionic conductivity of Nafion/[MimHE]Cl/PA is the second highest, and the ionic conductivity of Nafion/[MimCM]Cl/PA is the lowest. The proton conduction mechanisms for water-swelled electrolyte membranes can be summarized as two types, proton hopping (Grotthuss mechanism) and matrix transport (vehicular mechanism).^{32,33} Cho et al. reported that ILs in Nafion composite membranes behave like water by a hopping mechanism.³⁴ Upon addition into Nafion, phosphoric acid was protonated by the protons of Nafion and generated H_4PO_4^+ . The relatively low concentration of H_2PO_4^- reduced the self-ionization of the phosphoric acid.³⁵ Furthermore, the hydrogen-bonding network of phosphoric acid for hopping conductivity is weakened and results in a low conductivity. Compared with the Nafion/PA composite membranes, the protic ILs enhance the affinity of phosphoric acid in the Nafion matrix, resulting in more phosphoric acid incorporated with Nafion to form a hydrogen-bonding network for hopping conductivity.

The variation in conductivity for the three Nafion/IL/PA composite membranes is due to the different functional groups in the IL molecules. The amino group in [MimAE]Cl can be protonated by the protons of Nafion and phosphoric acid, which promotes the self-ionization of phosphoric acid and improves the conductivity. For [MimCM]Cl, the carboxyl group may release protons and reduce the self-ionization of phosphoric acid. The neutral hydroxyl group in [MimHE]Cl may have no influence in the self-ionization of phosphoric acid. Importantly, with the exception of the type of ILs, the ionic conductivity of the composite membranes is also dependent on the content of the ILs. As shown in Figure 3, the ionic conductivities of Nafion/20 wt % [MimHE]Cl/PA and Nafion/20 wt % [MimCM]Cl/PA are both higher than Nafion/10 wt % [MimHE]Cl/PA and Nafion/10 wt % [MimCM]Cl/PA, respectively. This indicates that the ionic conductivity is increased with the increasing content of the ILs for the same type of ILs. We proposed that this result is due to the fact that more phosphoric acid is incorporated in the composite membranes with the increased content of the ILs.

To investigate the impact of phosphoric acid in the composite membranes, the conductivity of the Nafion/IL composite membranes without phosphoric acid is shown in Figure 4. All three of the Nafion/IL composite membranes

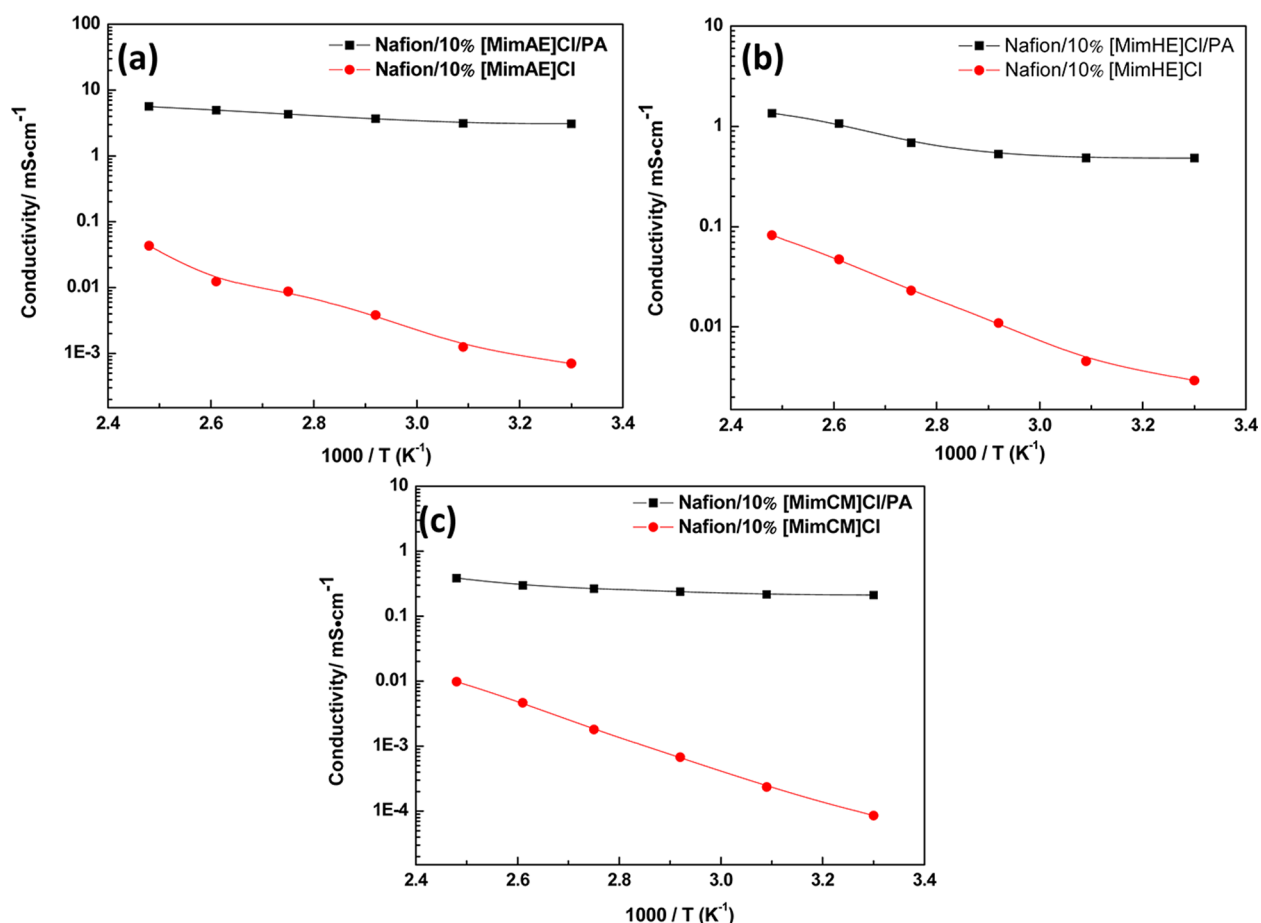


Figure 4. Comparison of the conductivity for the Nafion/IL/PA membranes and Nafion/IL membranes as a function of temperature.

exhibit poor conductivities, which are nearly 2 to 3 orders of magnitude smaller than that of the Nafion/IL/PA composite membranes. Additionally, the conductivities of the Nafion/IL composite membranes also show a relatively higher temperature dependency. We believe that the added phosphoric acid can supply more protons and also decrease the viscosity of the ILs in Nafion. The enhanced mobility of protons by the decreased viscosity of the ILs results in the increased ionic conductivity.

Structure and Morphology of the Composite Membranes. SAXS measurements were conducted to examine the structures of the composite membranes. In general, Nafion consists of two incompatible parts: a hydrophobic fluorocarbon backbone and a hydrophilic sulfonic acid side chain. Thus, the unique structure of the Nafion membrane is constituted by a fluorocarbon domain to maintain mechanical stability and an ionic domain to favor ion mobility.³⁶ The SAXS spectra of swollen Nafion membranes were recently recorded and distinguished the matrix knee at $q \sim 0.035 \text{ \AA}^{-1}$ and the ionomer peak at $0.1\text{--}0.2 \text{ \AA}^{-1}$.³⁷ The matrix knee generally appears as a shoulder peak and reveals the crystallinity of Nafion or the forms of microcrystal in the hydrophobic fluorocarbon phase. Given as a fingerprint, the ionomer peak is generating from the patterns of ionomer domains or their dimensional distribution and indicates the hydrophilic–hydrophobic phase separation.³⁷ In addition, the mean distance, $d = 2\pi/q$, of the connected ionic clusters can be calculated from the position q of the ionomer peak.²¹ Figure 5 shows the SAXS spectra for the pristine Nafion membrane and the Nafion/IL/

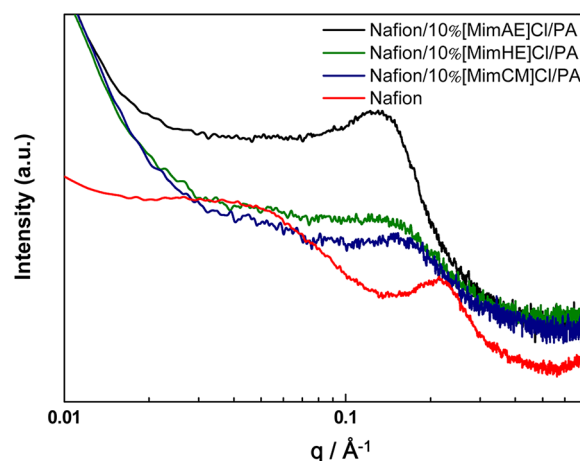


Figure 5. Small-angle X-ray scattering (SAXS) intensity as a function of the scattering vector q for Nafion and Nafion/IL/PA composite membranes containing 10 wt % of the corresponding ILs.

PA composite membranes containing 10 wt % of the corresponding ionic liquids after immersion in phosphoric acid. The pristine Nafion membrane shows two peaks at 0.0416 and 0.216 \AA^{-1} , corresponding to the matrix knee and ionomer peak, respectively. With the incorporation of ionic liquids and phosphoric acid, the matrix peaks vanished and the ionomer peaks shifted to a lower q , indicating the decline in the crystallinity of the Nafion matrix and the enlargement of the mean distance between the ionic domains. This means that the

ionic domains containing ionic liquids and phosphoric acids are larger than the polar domains of Nafion. The Nafion/[MimAE]Cl/PA composite membrane at $q = 0.132 \text{ \AA}^{-1}$ ($d = 47.6 \text{ \AA}$) has the maximum domain separation, resulting in the highest ionic conductivity among the three composite membranes. The ionomer peaks of the Nafion/[MimHE]Cl/PA and Nafion/[MimCM]Cl/PA membranes can be observed at $q = 0.143 \text{ \AA}^{-1}$ ($d = 43.9 \text{ \AA}$) and $q = 0.162 \text{ \AA}^{-1}$ ($d = 38.8 \text{ \AA}$), respectively. The composite membranes are thus separated into a hydrophobic fluorocarbon phase and an ionic phase containing ionic liquids and phosphoric acids. Furthermore, as shown in Figure 5, the insertion of [MimHE]Cl and [MimCM]Cl leads to a significant broadening of the ionomer peak compared to that of [MimAE]Cl. This result indicates that [MimAE]Cl can swell the Nafion structure more homogeneously than [MimHE]Cl and [MimCM]Cl.³⁸ The heterogeneous distributions of [MimHE]Cl and [MimCM]Cl in the Nafion matrix result in a relatively poor conductivity compared to [MimAE]Cl.

SEM images (Figure 6) show the surface and cross-section morphologies of the pristine Nafion and Nafion/IL/PA composite membranes. The surface and cross-section views of

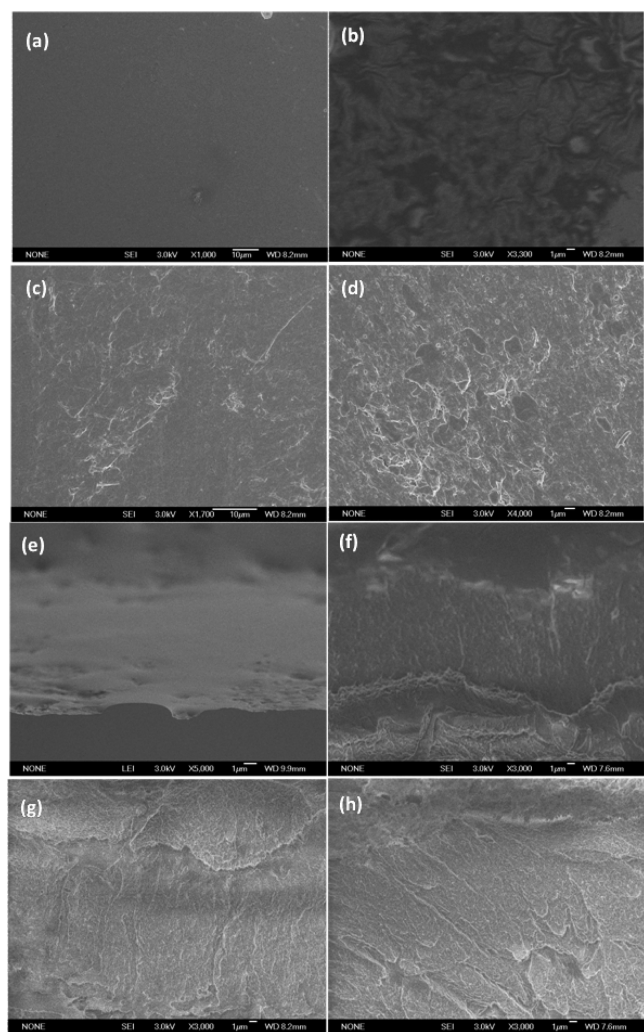


Figure 6. SEM images of the surface and cross-sections of Nafion (a, e), Nafion/10% [MimAE]Cl/PA (b, f), Nafion/10% [MimHE]Cl/PA (c, g), and Nafion/10% [MimCM]Cl/PA (d, h).

Nafion look uniform and dense. When ionic liquids and phosphoric acid were added into the Nafion matrix, the morphologies of the composite membranes became particularly wrinkled and spongy. It is important to note that no large agglomerates are visible on the surface or through the section; this means that the ionic liquids and phosphoric acid can be dispersed homogeneously in the Nafion matrix thereby maintaining submicrometric dimensions.

Thermal Stability. Figure 7 shows the thermogravimetric (TG) curves of the pristine Nafion and the composite

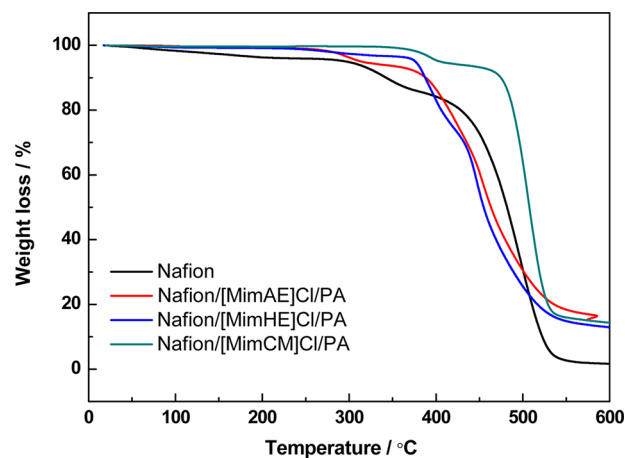


Figure 7. TGA curves for Nafion and Nafion/IL/PA composite membranes containing 10 wt % of the corresponding ionic liquids.

membranes with 10 wt % ionic liquids. The decomposition temperature (T_d) values of all of the composite membranes are higher than 250 °C and are sufficient for conductivity measurements. It is seen that the T_d values of all of the Nafion/IL/PA composite membranes are higher than that of Nafion. The increased thermal stability of the Nafion/IL/PA composite membranes indicates that there are strong electrostatic interactions between the sulfonic groups of Nafion and the imidazolium cations of ionic liquids.²² For pure Nafion, the first weight loss corresponds to water evaporation. The addition of ionic liquids and phosphoric acid reduced the water content in the composite membranes, resulting in an inconspicuous degradation before 300 °C. Figure 8 shows the derivative

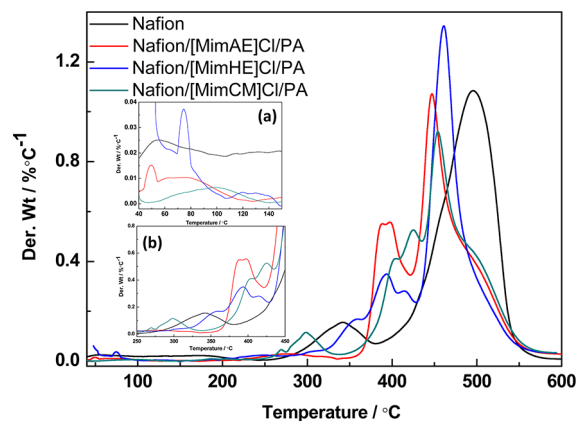


Figure 8. Derivative of the TG profiles for Nafion and Nafion/IL/PA composite membranes. The insets show the derivative in the temperature ranges of 40–150 °C (a) and 250–450 °C (b).

Table 1. Values for the Onset, $T_{d,onset}$ ($^{\circ}\text{C}$), of the Nafion/IL/PA Composite Membranes and Pristine Nafion

Nafion/[MimAE]Cl/PA	Nafion/[MimAE]Cl/PA	Nafion/[MimAE]Cl/PA	Nafion
288	366	327	351

%/dT from 40 to 600 $^{\circ}\text{C}$. As shown in inset a, the loss of water occurs between 40 and 150 $^{\circ}\text{C}$. Ignoring the disturbance in the samples of Nafion/[MimAE]Cl/PA and Nafion/[MimHE]Cl/PA, the pristine Nafion membranes generate water loss at the lowest temperature around 55 $^{\circ}\text{C}$. However, for samples Nafion/[MimAE]Cl/PA, Nafion/[MimHE]Cl/PA, and Nafion/[MimCM]Cl/PA, the temperature of the water evaporation is around 70, 130, and 100 $^{\circ}\text{C}$, respectively. The Nafion/[MimHE]Cl/PA composite membrane with the highest temperature for water evaporation results from the strong hydrogen-bond interactions between the hydroxyl groups and water molecules. Compared with that of the pristine Nafion, the hydrophilic domains of doped composite membranes are filled with ILs and result in a low hydration. The weight loss due to water evaporation is about 1, 0.3, 0.5, and 2.5 wt % for Nafion/[MimAE]Cl/PA, Nafion/[MimHE]Cl/PA, Nafion/[MimCM]Cl/PA, and pristine Nafion, respectively. From the derivative dwt %/dT shown in insert b of Figure 8, the initial temperature of decomposition, $T_{d,onset}$, is determined and listed in Table 1. Pristine Nafion can be thermally stable up to about 280 $^{\circ}\text{C}$, whereas for the Nafion/IL/PA composite membranes, the decomposition temperatures are all over 300 $^{\circ}\text{C}$. Therefore, the added ionic liquids and phosphoric acid decrease the water content in Nafion membranes and work as plasticizers to increase the thermal stability of Nafion matrix.

CONCLUSIONS

Three protic imidazolium ILs with different functional groups, amino, hydroxyl, and carboxyl, were successfully incorporated with Nafion membranes by a solution-casting method. The obtained Nafion/IL membranes were further immersed in concentrated phosphoric acid to fabricate high-temperature proton-conducting Nafion/IL/PA membranes. The incorporated protic ionic liquids enhance the doping of phosphoric acid and result in a relatively high ionic conductivity. When 10 wt % [MimAE]Cl was added into Nafion, the composite membrane exhibits an ionic conductivity of 6.0 mS/cm at 130 $^{\circ}\text{C}$ under anhydrous conditions. SAXS results demonstrated that [MimAE]Cl can disperse in Nafion matrix more homogeneously than [MimHE]Cl and [MimCM]Cl, which contributed its better ionic conductivity. According to the TG results, the water content of the Nafion/IL/PA composite membranes are reduced because the ionic domains are filled with ionic liquids, and the temperatures of thermal degradation are relatively raised. The incorporated ionic liquids and phosphoric acid can act as plasticizers and increase the thermal stability of the Nafion matrix. Thus, the Nafion/IL/PA composite membranes have great potential to be applied as high-temperature membranes for PEMFCs.

AUTHOR INFORMATION

Corresponding Author

*E-mail: lqzheng@sdu.edu.cn. Phone: +86-531-88361528. Fax: +86-531-885647.

Notes

The authors declare no competing financial interest.

ACKNOWLEDGMENTS

The authors are grateful to the National Basic Research Program (2013CB834505), the National Natural Science Foundation of China (no. 91127017), the Specialized Research Fund for the Doctoral Program of Higher Education of China (no. 20120131130003), and the Shandong Provincial Natural Science Foundation of China (ZR2012BZ001).

REFERENCES

- (1) Savadogo, O. *J. New Mater. Electrochem. Syst.* **1998**, *1*, 47–66.
- (2) Savadogo, O. *J. Power Sources* **2004**, *127*, 135–161.
- (3) Ye, Y. S.; Cheng, M. Y.; Tseng, J. Y.; Liang, G. W.; Rick, J.; Huang, Y. J.; Chang, F. C.; Hwang, B. J. *J. Mater. Chem.* **2011**, *21*, 2723–2732.
- (4) Yasuda, T.; Nakamura, S.; Honda, Y.; Kinugawa, K.; Lee, S. Y.; Watanabe, M. *ACS Appl. Mater. Interfaces* **2012**, *4*, 1783–1790.
- (5) Higashihara, T.; Matsumoto, K.; Ueda, M. *Polymer* **2009**, *50*, 5341–5357.
- (6) Xu, K.; Chanthad, C.; Gadinski, M. R.; Hickner, M. A.; Wang, Q. *ACS Appl. Mater. Interfaces* **2009**, *1*, 2573–2579.
- (7) Lin, B. C.; Cheng, S.; Qiu, L. H.; Yan, F.; Shang, S. M.; Lu, J. M. *Chem. Mater.* **2010**, *22*, 1807–1813.
- (8) Baker, A. M.; Wang, L.; Advani, S. G.; Prasad, A. K. *J. Mater. Chem.* **2012**, *22*, 14008–14012.
- (9) Feng, K.; Tang, B. B.; Wu, P. Y. *ACS Appl. Mater. Interfaces* **2013**, *5*, 1481–1488.
- (10) Mauritz, K. A.; Moore, R. B. *Chem. Rev.* **2004**, *1004*, 4535–4585.
- (11) Banerjee, S.; Curtin, D. E. *J. Fluorine Chem.* **2004**, *125*, 1211–1216.
- (12) Souzy, R.; Ameduri, B. *Prog. Polym. Sci.* **2005**, *30*, 644–687.
- (13) Neves, L. A.; Sebastião, P. J.; Coelho, I. M.; Crespo, J. G. *J. Phys. Chem. B* **2011**, *115*, 8713–8723.
- (14) Li, Q.; He, R.; Jensen, J. O.; Bjerrum, N. J. *Chem. Mater.* **2003**, *15*, 4896–4915.
- (15) Bonhôte, P.; Dias, A. P.; Papageorgiou, N.; Kalyanasundaram, K.; Grätzel, M. *Inorg. Chem.* **1996**, *35*, 1168–1178.
- (16) Di Noto, V.; Piga, M.; Giffin, G. A.; Lavina, S.; Smotkin, E. S.; Sanchez, J. Y.; Iojoiu, C. *J. Phys. Chem. C* **2012**, *116*, 1361–1369.
- (17) Di Noto, V.; Piga, M.; Giffin, G. A.; Lavina, S.; Smotkin, E. S.; Sanchez, J. Y.; Iojoiu, C. *J. Phys. Chem. C* **2012**, *116*, 1370–1379.
- (18) Di Noto, V.; Negro, E.; Sanchez, J. Y.; Iojoiu, C. *J. Am. Chem. Soc.* **2010**, *132*, 2183–2195.
- (19) Martinez, M.; Molmeret, Y.; Cointeaux, L.; Iojoiu, C.; Leprêtre, J. C.; Kissi, N. E.; Judeinstein, P.; Sanchez, J. Y. *J. Power Sources* **2010**, *195*, 5829–5839.
- (20) Neves, L. A.; Benavente, J.; Coelho, I. M.; Crespo, J. G. *J. Membr. Sci.* **2010**, *347*, 42–52.
- (21) Baek, J. S.; Park, J. S.; Sekhon, S. S.; Yang, T. H.; Shul, Y. G.; Choi, J. H. *Fuel Cells* **2010**, *10*, 762–769.
- (22) Yang, J. S.; Che, Q. T.; Zhou, L.; He, R. H.; Savinell, R. F. *Electrochim. Acta* **2011**, *56*, 5940–5946.
- (23) Mistry, M. K.; Subianto, S.; Choudhury, N. Y.; Dutta, N. K. *Langmuir* **2009**, *25*, 9240–9251.
- (24) Wainright, J. S.; Wang, J. T.; Weng, D.; Savinell, R. F.; Litt, M. J. *Electrochem. Soc.* **1995**, *142*, L121–L123.
- (25) Wasmus, S.; Valeriu, A.; Mateescu, G. D.; Tryk, D. A.; Savinell, R. F. *Solid State Ionics* **1995**, *80*, 87–92.
- (26) Li, Q.; Hjuler, H. A.; Bjerrum, N. J. *Electrochim. Acta* **2000**, *45*, 4219–4226.
- (27) Yan, L. M.; Zhu, S. H.; Ji, X. B.; Lu, W. C. *J. Phys. Chem. B* **2007**, *111*, 6357–6363.

- (28) Bates, E. D.; Mayton, R. D.; Ntai, I.; Davis, J. H. *J. Am. Chem. Soc.* **2002**, *124*, 926–927.
- (29) Zhou, X. S.; Wu, T. B.; Ding, K. L.; Hu, B. J.; Hou, M. Q.; Han, B. X. *Chem. Commun.* **2009**, *14*, 1897–1899.
- (30) Sun, J.; Zhang, S. J.; Cheng, W. G.; Ren, J. Y. *Tetrahedron Lett.* **2009**, *49*, 3588–3591.
- (31) Liu, D.; Gui, J. Z.; Zhu, X.; Song, L. J.; Sun, Z. L. *Synth. Commun.* **2007**, *37*, 759–765.
- (32) Noda, A.; Susan, M. A. B. H.; Kudo, K.; Mit-sushima, S.; Hayamizu, K.; Watanabe, M. *J. Phys. Chem. B* **2003**, *107*, 4024–4033.
- (33) Matsuoka, H.; Nakamoto, H.; Susan, M. A. B. H.; Watanabe, M. *Electrochim. Acta* **2005**, *50*, 4015–4021.
- (34) Cho, E. K.; Park, J. S.; Sekhon, S. S.; Park, G. G.; Yang, T. H.; Lee, W. Y.; Kim, C. S. *J. Electrochem. Soc.* **2009**, *156*, B197–B202.
- (35) Savinell, R.; Yeager, E.; Tryk, D.; Landau, U.; Wainright, J.; Weng, D.; Lux, K.; Litt, M.; Rogers, C. *J. Electrochem. Soc.* **1994**, *141*, L46–L48.
- (36) Gebel, G. *Polymer* **2000**, *41*, 5829–5838.
- (37) Gebel, G.; Diat, O. *Fuel Cells* **2005**, *5*, 261–276.
- (38) Sood, R.; Iojoiu, C.; Espuche, E.; Gouanvé, F.; Gebel, G.; Mendil-Jakani, H.; Lyonard, S.; Jestin, J. *J. Phys. Chem. C* **2012**, *116*, 24413–24423.